MULTI-OBJECTIVE DEPARTURE TRAJECTORY OPTIMISATION OF COMMERCIAL AIRCRAFT ON ENVIRONMENTAL IMPACTS

MULTI-OBJECTIVE DEPARTURE TRAJECTORY OPTIMISATION OF COMMERCIAL AIRCRAFT ON ENVIRONMENTAL IMPACTS

Mengying Zhang[(1)], Antonio Filippone[(2)], Nicholas Bojdo[(3)]

[(1)]The University of Manchester, United Kingdom, M13 9PL, mengying.zhang@manchester.ac.uk
[(2)]The University of Manchester, United Kingdom, M13 9PL, a.filippone@manchester.ac.uk
[(3)]The University of Manchester, United Kingdom, M13 9PL, nicholas.bojdo@manchester.ac.uk

KEYWORDS: trajectory optimisation, noise, emissions, genetic algorithm

ABSTRACT:

This research systematically evaluates the impacts on the environment regarding aircraft noise and exhaust emissions, aiming at identifying the potential optimal aircraft flight trajectories with respect to different objectives. A trajectory optimisation method based on genetic algorithms is developed to cover a wider range of formations of optimisation objectives without strict requirements of problem formulation. To solve the low computational efficiency problems caused by a large number of free parameters, a new parameterization approach is applied to discretize the dynamics equations. Furthermore, a dynamic bound method is proposed to define the upper and lower bounds of free parameters to avoid threatening potential search space. By applying the proposed method, numerical simulation is conducted addressing different optimisation tasks with required operational constraints. Results reveal that the proposed method is applicable, reliable and flexible to solve multi-objective optimisation problems.

1. INTRODUCTION

Air transportation is one of the most significant traffic services in the word. While making a balance between maximising the utilisation of aviation growth and minimising the environmental impact of aircraft operations might be drastic and critical. With the rapid growth of commercial aviation, there is an increasing public concern on the environmental effects of air travel, such as noise and air pollution. Currently, commercial aircraft follow prescribed procedures during departure and approach, such as Standard Instrumental Departures (SIDs) and Standard Terminal Arrival Routes (STARs)[1], [2]. Moreover, in order to reduce noise impact for departing aircraft, the ICAO proposed two general families of procedures: the Noise Abatement Departure Procedure (NADP) 1 to reduce noise in zones close to the airport and NADP 2 to reduce noise in zones far away from the airport [1]. However, such standard procedures are designed for a bunch of different types of aircraft under different flight conditions, which means they need to be adapted to specific aircraft and airport, otherwise, they might not always be optimal in terms of environmental impacts optimisation.

The possibility of using trajectory optimisation methods to minimise noise and pollutant emissions has generated wide interest during the past few years. Visser et al. [3], [4] developed a trajectory optimisation tool named NOISHHH, integrating a noise model, a geographic information system and a dynamics trajectory optimisation algorithm. The core of the trajectory optimisation tool is the direct optimal control problem solver which implements the collocation method [5] to convert the continuous optimal control problem into a finite-dimensional nonlinear programming problem. A similar algorithm has also been adopted in the optimisation methodology developed by Hartjes et al. [6], developed for multi-event aircraft trajectories. Moreover, Prats et al. [7], [8] applied a multi-criteria optimisation strategy with the lexicographic-egalitarian technique to minimise the noise annoyance impact in noise sensitive areas. In the research of Khardi et al. [9], the direct method was considered to be more adapted for solving trajectory optimisation problem minimising aircraft noise at reception points around airports compared with the indirect method.

All the methods mentioned above fall into the category of either gradient-based or derivative-based methods. However, these kinds of numerical algorithms have their own limitations when dealing with optimisation problems for discontinuous models. This means that their objective function and constraints need to be differentiable. With the increasing complexity and integration of current optimisation problem formulation, not all integrated problems can be

constructed with continuous models and functions with continuous derivatives. This has led to a boom of heuristic algorithms that are generally not computationally competitive at present, but do not need gradients of functions, making them more suitable and flexible to search global optimal solutions to the specific types of optimisation problems described above. Torres et al. [10] studied the implementation of a multi-objective mesh adaptive direct search (multi-MADS) method to minimise noise and NO_x emissions for departing aircraft. Similarly aimed at minimising noise impact for arrival trajectories, Yu et al. [11], [12] conducted state parameterization with Bernstein polynomials to transform the infinite-dimensional optimal control problem into a finite-dimensional parametric optimisation problem. In his research, a genetic algorithm was employed to optimise the parameters within the search space to obtain optimal trajectory both in vertical and lateral plane. Similarly, Hartjes and Visser [13] applied the genetic optimisation algorithms to design departure flight path focusing on noise abatement and NO_x reduction. However, genetic algorithms usually have the disadvantage of being computationally expensive, due to the need for a large number of free parameters for the problem evaluation.

In this study, a trajectory optimisation method based on genetic algorithms is developed to cover a wider range of formations of optimisation objectives without the strict requirements of problem formulation. The aircraft flight mechanics, aerodynamics, propulsion and acoustics models used in this work are based on the configuration of Airbus A320-211 with CFM56 engines. To solve the low computational efficiency problems caused by a large number of free parameters, a new parameterization approach is applied to discretize the dynamics equations on the vertical and lateral motion planes. Furthermore, a dynamic bound method is proposed to define the upper and lower bounds of the free parameters to replace their prescribed fixed values, for the reason of not threatening the potential search space and satisfying the majority of the path constraints.

The rest of this paper will be structured as follows. First of all, the problem statement including the trajectory optimisation problem formulation and the objective model will be presented. Next, the procedures of trajectory decoupling, segmentation and state parameterization are described, followed by the dynamic bound technique. Subsequently, a numerical example and its results are presented. Finally, the paper is concluded with the discussion and future plan.

2. METHODOLOGY

2.1 Aircraft Dynamics Model

In order to minimize the environmental impact, a constrained optimal control problem has been developed to define the trajectory optimisation process. Components including the aircraft flight dynamics model, constraints of flight configuration and safety issues, cost functions of different concerns are introduced in the following sections.

In general, an aircraft can be modelled as a rigid body with varying mass, aerodynamic, propulsive and gravitational forces. Several assumptions are made in order to simplify the problem: (1) the earth is considered to be flat and non-rotational, (2) no wind is presented in this work, (3) all force acting on the aircraft go through its centre of gravity, (4) the angle between the engine thrust F_N and the longitudinal axis of the aircraft is assumed to be equal to zero, (5) the angle of attack α is small. Then a 3DOF flight dynamics model with a set of differential algebraic equations associated with a variable mass m is as following.

$$\begin{cases} \dot{V} = \dfrac{F_N - mg\sin\gamma - D}{m} \\ \dot{\gamma} = \dfrac{L\cos\mu - mg\cos\gamma}{mV} \\ \dot{\chi} = \dfrac{L\sin\mu}{mV\cos\gamma} \\ \dot{x} = V\cos\gamma\sin\chi \\ \dot{y} = V\cos\gamma\cos\chi \\ \dot{h} = V\sin\gamma \\ \dot{m} = -f \end{cases} \tag{1}$$

where V is the true airspeed, γ is the flight path angle, χ is the heading angle, μ is the bank angle, x , y , h are the state variables to describe the location of the aircraft in the three dimensional space, f is the fuel flow rate. Based on the comprehensive flight mechanics software FLIGHT[14]–[16], the chosen model to calculate the engine thrust F_N and fuel flow rate f are expressed as

$$F_N = F_N(h, Ma, N_1) \quad (2)$$

$$f = f(h, Ma, N_1) \quad (3)$$

where Ma is the Mach number, $N_1 \in [70\%, 103\%]$ is the engine rpm.
The aerodynamic lift L and drag D are given by

$$L = \frac{1}{2}\rho V^2 C_L S \quad (4)$$

$$D = \frac{1}{2}\rho V^2 C_D S \quad (5)$$

where ρ is the atmospheric density, S is reference area, C_L and C_D are the lift coefficient and drag coefficient respectively both of which can be obtained from the FLIGHT with required aircraft configuration and motion parameters as well.

2.2 Parameterization

This section will introduce the method adopted to discrete the trajectory in the time interval. Several assumptions are made first for decoupling the motions between horizontal and vertical planes.
Firstly, the force normal to the flight path is assumed in equilibrium. This assumption $\dot{\gamma} = 0$ is made so that the lift and the portion of the weight normal to the flight path is balanced during each time step of the climb procedure, which leads to

$$\dot{\gamma} = \frac{L\cos\mu - mg\cos\gamma}{mV} = 0 \quad (6)$$

Then, lift coefficient is calculated by the Eq.7.

$$C_L = \frac{mg\cos\gamma}{\frac{1}{2}\rho V^2 S\cos\mu} \quad (7)$$

After assuming a parabolic drag polar, the drag force could be derived by the Eq. 8.

$$D = (C_{D0}(h,V) + k(h,V)C_L{}^2)\cdot\tfrac{1}{2}\rho V^2 S \quad (8)$$

where C_{D0} and k are the parabolic drag polar coefficients. Similarly, small value as it is, the angle of attack α can be derived from the linear equation

$$\alpha = \frac{C_L - C_{L0}(h,V)}{C_{L\alpha}(h,V)} \quad (9)$$

where C_{L0} and $C_{L\alpha}$ are the zero lift coefficient and lift curve slope respectively. Then α will no longer be a control variable.
However, since $\dot{\gamma} = 0$ is assumed within each time step, the value of flight path angle γ in each time step should be defined as an input parameter, which makes γ a control variable. Thus we have a state variable vector $\mathbf{x} = [V, \chi, x, y, h, m]^T$, and a new control vector $\mathbf{u} = [N_1, \gamma, \mu]^T$ .Then the Eq. 1 can be decoupled in the vertical plane and horizontal plane respectively in Eqs. 10-11.

$$\text{Horizontal:} \quad \begin{cases} \dot{\chi} = \dfrac{g\tan\mu}{V} \\ \dot{x} = V\cos\gamma\sin\chi \\ \dot{y} = V\cos\gamma\cos\chi \end{cases} \quad (10)$$

$$\text{Vertical:} \quad \begin{cases} \dot{V} = \dfrac{F_N - mg\sin\gamma - D}{m} \\ \dot{h} = V\sin\gamma \\ \dot{m} = -f \end{cases} \quad (11)$$

2.2.1 Horizontal Parameterization

Most departing commercial aircraft will follow departure routes that have been based on the modern navigation technology. Requirements such as to make sufficient use of runway capacity, to maintain safe separation between departures, to avoid the increase in traffic control workload and to mitigate new population exposed to noise have been taken into consideration, giving rise to a concentration of pre-programmed departure procedure, especially for the lateral tracks. Among those horizontal track parameterization methods, waypoints are usually used to define the departure routes. The lateral tracks can be expressed by a series of waypoints enable to construct the flight path between each two waypoints. Trajectories models defined by spline interpolation have been developed and introduced[17]. From the easiest straight line segments to the more complex piecewise cubic interpolation, different types of splines have been applied either to connect each

waypoint or to construct the flight path along the direction guided by the series of waypoints.
In this study, lateral track is expressed by a sequence of waypoints and legs. Two different types of legs: track-to a-fix (TF) legs and radius-to-a-fix (RF) legs - are preferred. This means the lateral trajectories can be constructed with straight legs and constant radius turns[13], [18], [19]. The arc one is commonly used for connecting two straight legs which have different heading angles (see Fig. 1). Assume the ground track is divided by n segments, then to define a constant radius turn, the required parameters are the radius R_i and the angle of fly-by-turn θ_i , $i=1,2,...,n$. Note that the angle of fly-by-turn is equal to the absolute value of the change of the heading angle $\theta_i = |\Delta\chi_i|$.

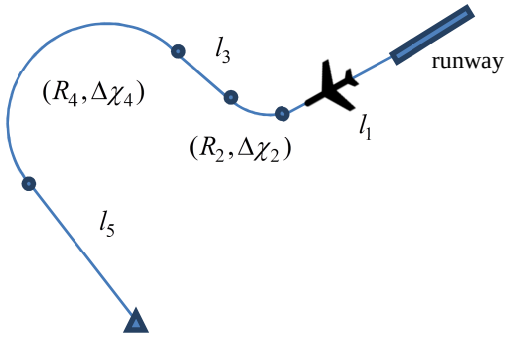

Figure 1. Example Ground tracks with straight legs and constant radius turns with $n=5$

With a given radius R and the local true airspeed V , the control variable bank angle μ are able to be derived from Eqs. 12-13.

$$m\frac{V^2}{R} = mg|\tan\mu| \tag{12}$$

$$\mu = \pm\tan^{-1}(\frac{V^2}{gR}) \tag{13}$$

To define a straight leg, only the length of the leg l is needed because the heading angle stays constant with the one at the last waypoint, which lead to a zero bank angle during the straight segment.

$$\mu = 0 \tag{14}$$

Thus the coordinate of the waypoints $(x_i, y_i), i \le n-1$, can be expressed by the ground track parameters. For straight segment,

$$\begin{cases} x_i = x_{i-1} - l_i \sin\chi_{i-1} \\ y_i = y_{i-1} + l_i \cos\chi_{i-1} \end{cases} \tag{15}$$

and for arc segment

$$\begin{cases} x_i = x_{i-1} - 2R_i \sin\left|\frac{\Delta\chi_i}{2}\right| \sin(\frac{\Delta\chi_i}{2} + \chi_{i-1}) \\ y_i = y_{i-1} + 2R_i \sin\left|\frac{\Delta\chi_i}{2}\right| \cos(\frac{\Delta\chi_i}{2} + \chi_{i-1}) \end{cases} \tag{16}$$

For a lateral track with fixed terminal point, only one more freedom need to be constrained to define the last two segments. To sum up, to construct a ground track with n segments, $(n+1)/2$ straight lines and $(n-1)/2$ arcs are needed to compose this ground track if the last segment is straight. Parameters to define this kind of ground track are shown in Tab. 1. The total number of the parameters required is given in Eq. 17.

$$N = (\frac{n+1}{2} - 1) + 2(\frac{n-1}{2} - 1) + 1 = \frac{3n-5}{2} \tag{17}$$

Table 1.Ground track parameters

segment	Parameter needed
1st	l_1
$i^{\text{th}} (i = 2,...,n-2)$	$(R_i, \Delta\chi_i)$ for the arcs
	l_i for the straight lines
$n-1^{\text{th}}$	R_{n-1}
n^{th}	none

2.2.2 Vertical Parameterization

2.2.2.1 Dynamic Variable Boundary

Before entering into the parameterization of the vertical flight path, a technique dealing with variables value range in this study will be presented first. In solving trajectory optimization problem, the application of constraints usually has more requirements to be considered. For both

derivative-based algorithms and non-based algorithms, state variables or free parameters are limited in some prescribed interval as is shown in Eq. 18.

$$x_{\min} \le x \le x_{\max} \tag{18}$$

Although the constraints are made for the aircraft to fly safely and reliably, to decide the lower and upper bounds of the variable depends much on transcendentally prescribed value, which may manually narrow or enlarge the search space of the original problem. Computational efficiency might also be affected when the range of search space is changed. As a consequence, an effective and efficient way to define the boundary of the variables and free parameters is of high importance, especially for the non-derivative algorithms (e.g. genetic algorithm). Unlike the direct or indirect methods to solve this optimisation problem, there are no dynamic constraints in the process of GA solving. As a consequence, solution space depends much on the search space made from prescribed boundary values of free parameters.

When applied in this study, the boundary values for control variables are no longer constants but change correspondently with real-time flight condition in each time step.

$$\begin{aligned} N_{1\min,i} &= N_1(D_{i-1}) \\ N_{1\max,i} &= 103\% \end{aligned} \tag{19}$$

For level flight segment,

$$\gamma_{\min,i} = 0^{\circ}, \gamma_{\max,i} = 0^{\circ} \tag{20}$$

For climb segment,

$$\begin{aligned} \gamma_{\min,i} &= 0^{\circ} \\ \gamma_{\max,i} &= \sin^{-1}\left(\frac{F_{N\max} - D_{i-1}}{m_{i-1}g} - \frac{1}{g}\left(\frac{dV}{dt}\right)_{i-1} \right) \end{aligned} \tag{21}$$

where $F_{N\max} = F_N(n_{1\max})$ at specific altitude and velocity, $\left(\frac{dV}{dt}\right)_{i-1} = F_{Ni-1} - m_{i-1}g - D_{i-1}$, subscript i denotes the i^{th} time step. Before each time step, a judgement will be made to assure the value of the control variables n_1 and γ are within their updated boundaries. Otherwise the variables need to be assigned reasonable values

$$N_{1,i} = N_{1\min,i} + \text{rand}(1) \times (N_{1\max,i} - N_{\min,i}) \tag{22}$$

$$\gamma_i = \gamma_{\min,i} + \text{rand}(1) \times (\gamma_{\max,i} - \gamma_{\min,i}) \tag{23}$$

2.2.2.2 Vertical Segmentation and Parameterization

The departure procedure can be separated into several segments of climb and acceleration. One possible schedule is shown in Fig. 2 with example parameter values. According to this flight operation sequence, two accelerations and two constant speed climb phases are taken into account. Those parameters that describe the climb profile and their effect on the noise perceived at the noise sensitive points and emission pollution are the major concerns we need to investigate.

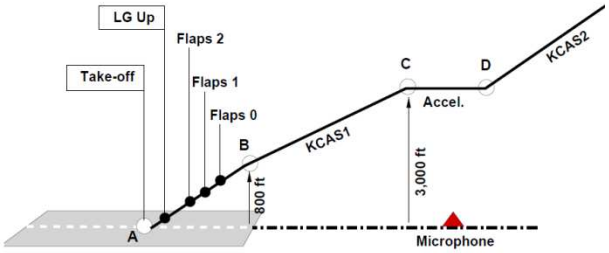

Figure 2. Take-off and climb-out[14]

A. Phase 1 : A-B

In segment AB, the aircraft is assumed to take off at maximum thrust until it reaches the point B where the speed V_B and altitude h_B are prescribed. As is shown in Fig. 2, during this phase, several operations of high lift device and the landing gear are usually taken into consideration. Yet these operations do exert little impact on the aircraft noise during the departure procedure. As a result we assume the aircraft operates under a clean configuration.

According to Eq. 6; the designed parameter in the AB phase are γ_A and V_B , where γ_A is the initial flight path angle, V_B is airspeed to be achieved at the end point B. A sequence is adopted to prevent the aircraft overfly the target terminal attitude and airspeed. If the terminal attitude h_B is achieved first, let $\gamma = \gamma_{\min} = 0^{\circ}$ and accelerate until the

aircraft reaches the prescribed airspeed V_B. From the other aspect, if V_B is reached first, let $\dot{V} = 0$, which leads to a constant speed climb to the target altitude .

Note that in reality, there are other parameters to define this segment. For example, according to the ICAO B procedure, the target altitude h_B could be any value between 800 feet to 1,500 feet, which makes it a free variable as well.

B. Phase 2: B-C

In this phase, the aircraft is assumed to climb at a constant speed. The terminal condition is to reach a final altitude $h_C = 3{,}000$ feet. During this constant speed climb phase, the only free parameter comes to be the flight path angle γ_B .

The procedure to solve this flight phase is listed below.

(1) Climb procedure starts from $\gamma_i = \gamma_B$

(2) Calculate the lift coefficient $C_{L,i}$ and drag D_i according to Eqs. 7-8.

(3)Since $\dot{V} = 0$, then the thrust can be obtained by

$$F_{N,i} = m_i g \sin\gamma_i + D_i(C_{D,i}, h_{i-1}, V_B) \tag{24}$$

(4) Induce γ_i , $C_{L,i}$, D_i and $F_{N,i}$ into the dynamics equation to obtain h_i and V_i in this time step.

Then go to the next step (1) and repeat the procedure until the final altitude h_C is reached.

C. Phase 3: C-D

In this phase, the aircraft is expected to do a level acceleration until it reaches a target speed V_D for the next climb. Therefore, the acceleration becomes the variable that decides the profile of this phase which could be control by the thrust or the engine rpm N_{1CD} . Assume the aircraft fly at a constant N_1 in this phase, a similar process is applied until the aircraft reaches its target airspeed.

D. Phase 4: D-E

As is shown in Fig. 2, after the acceleration in segment CD, one more climb segment has to be added to the vertical profile in order to achieve the terminal ground projection point (x_f, y_f) , which needs one parameter γ_D to define the climb rate of this segment. Procedure to constrain the flight path angle and engine rpm is the same as what has applied in the past segments. Constraints on final attitude according to the air traffic control requirements also need to be considered $h_D \le h_{\max}$, where $h_{\max}$ is the SID's upper limit (usually is 5,000 feet). Before reaching the ground target point or the altitude limit, the aircraft keeps climb with a constant speed. The problem of overpassing the altitude limit at the end of the trajectory can be solved by setting $\gamma = \gamma_{\min} = 0^o$ once it achieves 5,000 feet. Another problem that is somehow more difficult is that the constraints for thrust will be violated if the thrust derived from Eq. 24 is smaller than its lower bound $F_{N\min}$. To deal with this specific problem, the thrust setting is changed to be $F_N = F_{N\min}$. When $F_N < F_{N\min}$, the aircraft will accelerate under the new power setting until it reaches the terminal position. To sum up, seven free parameters are needed to decide a vertical climb profile

$$\mathbf{p}_{\text{vertical}} = [\gamma_A, V_B, \gamma_B, h_B, N_{1CD}, V_D, \gamma_D]^T \tag{25}$$

2.2.3 Coupling of Horizontal and Vertical Profiles

Previous sections present the trajectory parameterization of the horizontal and vertical profile respectively. From the Eqs.10-11, we understand that the departure trajectory can be parameterized through two sets of free parameters: $\mathbf{p}_{\text{horizontal}}$ to describe the lateral track on the ground and $\mathbf{p}_{\text{vertical}}$ to define vertical motion. Fig. 3 depicts the computational procedure of the 3D flight dynamics model. As is shown in Fig. 3, three control variables, namely the engine rpm N_1, the flight path angle γ and the bank angle μ , determine the motions on both horizontal and vertical planes.

2.4 Constraints

In this section, constraints that are taken into account are discussed. Firstly, path constraints for state variables are

$$V_{\text{stall}} < V \le 250\text{kt} \tag{26}$$

$$h_0 \le h \le h_{\max} \tag{27}$$

where V_{stall} is the stall speed, h_0 is the initial altitude. For a departure aircraft, neither descending nor deceleration should be permitted.

Thus, a couple of path constraints are introduced as

$$\gamma \geq 0 \tag{28}$$

$$\dot{V} \geq 0 \tag{29}$$

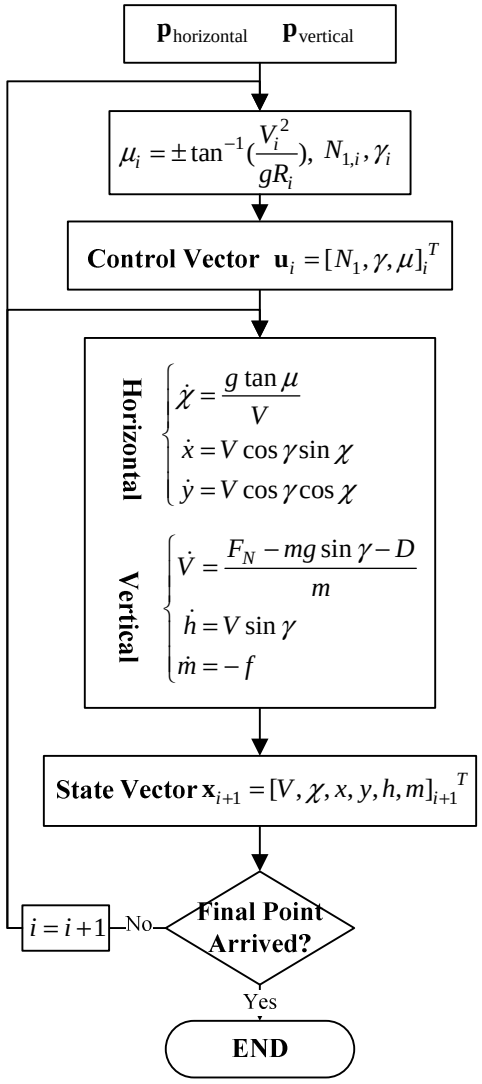

Figure 3. Computation procedure of 3D flight dynamics model

Secondly, for the control variables $\mathbf{u} = [N_1, \gamma, \mu]^T$, constraints on N_1 and γ could be obtained from Eqs. 24-26. However, as is discussed in Eqs. 13-14, the bank angle μ is an implicit rather than an explicit parameter in defining the ground track. As a result, the maximum bank angle of the aircraft could be deduced from the normal force equation

$$\mu \leq \tan^{-1}\sqrt{{n_{\max}}^2 - 1} \tag{30}$$

where $n = L/mg$ is the load factor.

Thirdly, the values of state and control variables of the dynamics system at the initial and final time are defined by the boundary conditions.

$$h(t_0) = h_0, x(t_0) = x_0, y(t_0) = y_0 \tag{31}$$

$$h(t_f) \leq h_{\max}, x(t_f) = x_f, y(t_f) = y_f \tag{32}$$

where (x_f, y_f) is usually chosen from the coordinates of the waypoints where the aircraft leaves controlled airspace of that typical airport.

Finally, other constraints on ground track include the length of the straight segment l, radius of the turn R, and the fly-by angle of each turn $|\Delta\chi|$. In general, the definition of $\mathbf{p}_{\text{horizontal}}$ should be set in coordinate with specific scenario. Yet, some similarities are shared in common. For example, in the first segment after take-off, usually no turns are permitted below a warning altitude h_{warning} [20]

$$l_1 \geq \cot\gamma_A h_{\text{warning}} \tag{33}$$

For the constraints of the radius, no sharp turns are allowed in the case of safety issue, therefore the constraint can be given by Eq. 34.

$$R = \frac{V^2}{g\tan\mu} \geq \frac{V^2}{g\sqrt{n_{\max}^2 - 1}} \tag{34}$$

2.5 Cost Function

Usually, different objectives such as flight duration, fuel burnt, noise, emissions and so on can be set as the optimisation objectives for the trajectory of an aircraft. For the assessment of environmental impacts, FLIGHT provides modules to evaluate different indexes. Usual aircraft environmental indexes, such as the EPNL (Effective Perceived Noise Level), SEL (Sound Exposure Level), $L_{A\max}$ (Maximum noise level), fuel consumption, CO_2 (carbon dioxide), NO_x (oxides of nitrogen) and so on are able to be calculated from this software.

Apart from the pure physical measurement quantifying environmental impacts, an integrated index to evaluate the financial cost of fuel

consumption and gaseous emissions is given in Eq. 36. Instead of summing up different objectives with the weighted method, this model transforms the fuel consumption , total amount of CO_2 emissions and NO_x emission under 3,000 feet[21] into a common metric from the aspect of the expenses to control the pollutants and energy consumed.

$$\mathrm{EC} = \mathrm{UC}_{\mathrm{fuel}} \cdot F + \mathrm{UC}_{\mathrm{CO}_2} \cdot \mathrm{CO}_2 + \mathrm{UC}_{\mathrm{NO}_x} \cdot \mathrm{NO}_x \quad (35)$$

where EC denotes the environmental cost for fuel and emissions, UC is the unit cost: for the fuel consumption, it is the unit jet fuel price; for the gaseous emissions, environment-related taxes are adopted.

3. NUMERICAL EXAMPLE

To demonstrate the capability of the method proposed, we consider one Airbus 320-211 aircraft departing toward the west off Runway 23R in Manchester Airport[21]. The closest community near the end of the Runway 23R/05L is Knutsford which will be annoyed by the aviation noise most. Thus, trajectory optimisation on departure for minimizing noise impact on Knutsford as well as local emission impact is the objectives.

$$J_1 = \mathrm{EPNL},\ J_2 = \mathrm{EC} \quad (36)$$

With the origin point located in the coordinate of Runway end 23R, the aircraft departures with initial conditions that takes off at $x_0 = -916.7118\mathrm{m}$, $y_0 = -399.5492\mathrm{m}$, $h_0 = 3\mathrm{m}$, $V_0 = 75\mathrm{m/s}$ with landing gear retracted and departure flaps selected. The finial conditions are selected from an existing SID, with final ground location fixed $x_f = -18119.1951\mathrm{m}$, $y_f = -16708.6863\mathrm{m}$, $h_f \le 1524\mathrm{m}$. Lateral track to be optimised can be segmented into five segments with three straight legs and two constant radius turns. Free parameters $\mathbf{p}_{\mathrm{horizontal}} = [l_1, R_2, \Delta\chi_2, l_3, R_4]^T$ and their bounds to define the ground track are listed in Tab. 2.

Table 2 Free parameters of ground track

segment number	Parameter
1	$l_1 \in [4000\mathrm{m}, 6000\mathrm{m}]$
2	$R_2 \in [2000\,\mathrm{m}, 3000\,\mathrm{m}]$, $\Delta\chi_2 \in [40^o, 90^o]$
3	$l_3 \in [2000\mathrm{m}, 4000\mathrm{m}]$
4	$R_4 \in [3000\,\mathrm{m}, 9000\,\mathrm{m}]$
5	none

Similarly, the free parameters for vertical profile $\mathbf{p}_{\mathrm{vertical}} = [\gamma_A, V_B, \gamma_B, h_B, N_{1CD}, V_D, \gamma_D]^T$ and their initial value range are shown in Tab. 3. Note that a reference value (i.e. 2.8^o) according to the existing SID is adopted for γ_D in order to decrease dimension of the search space. Then we have six free parameters to construct the vertical profile.
Therefore, a 3D departure trajectory is fully described with 11 free parameters. Due to the discrete formulation of this optimal control problem, functions of objectives and constraints are not derivable, which leads to a preference to use algorithms that do not need any gradient information. For this reason, a fast and elitist multi-objective genetic algorithm (NSGA-II)[22] is adopted as the optimiser.

Table 3. Vertical profile parameters

Parameters	Lower bound	Upper bound
γ_A	4^o	12^o
V_B	80m/s	100m/s
γ_B	4^o	12^o
h_B	243.84m	457.2m
n_{1CD}	86%	103%
V_D	100m/s	128.6m/s
γ_D	2.8^o	2.8^o

4. RESULTS

The example presents the departure trajectory optimisation aiming at minimizing Effective Perceived Noise Level (EPNL) and environmental cost for fuel consumptions and emissions (EC) in the 3D space. Before proceeding to the result, a reference trajectory is randomly picked as the baseline for the purpose of performance comparison.

The comparison result of the four representative cases, namely the reference one (case1),, the optimal solution (case2), EPNL-optimal case (case3), and EC-optimal case (case4), are summarized in Tab. 4. . Although time and distance *d* were not considered as the optimisation objectives in this example, they are included in Tab. 4 as the performance indicator for

the four cases. Fig.4 illustrates the comparison of their ground tracks.

Table 4. Comparison for the optimised trajectories and the baseline

Case	Time(s)	d (km)	ΔEPNL(%)	ΔEC(%)
1	360.3607	35.1932	/	/
2	309.3725	30.0413	-3.6900	-9.1161
3	280.3972	30.1672	-7.8633	-2.8634
4	271.0264	27.8373	+8.1540	-12.0977

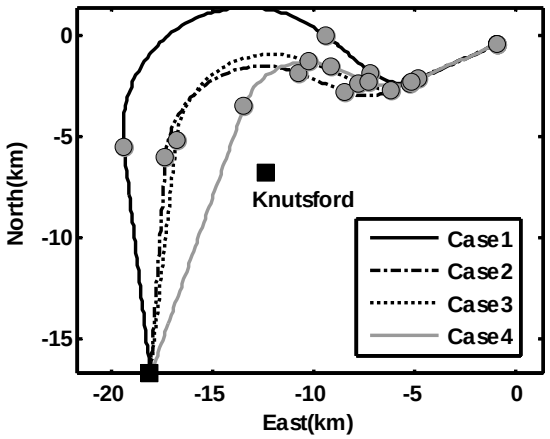

Figure 4. Departure ground track comparison

With the comparison between the values of bio-objectives, the multi-objectives nature of the problem is demonstrated. The extreme points of the Pareto solutions, case 3 and case 4, exhibit significant difference on the environmental indexes. Regarding the EPNL objective, both case 2 and case 3 have a progress in reduce noise impact (-3.6900% and -7.8633% respectively). By comparing the ground tracks of these two cases, it is clear that in both cases, a relatively early turn with larger radius is preferred when the aircraft circumvents the Knutsford area, which increases the receiver-to-source-distance and reduces the sound energy received. Case 4, in the contrary, flies much closer to the noise sensitive area resulting in a higher noise level compared with other three cases. However, it is not always true that the further aircraft moves away from the receiver the less annoyance it will cause. It is shown in the baseline trajectory that though the ground track is the furthest among others, its EPNL is not the lowest.

Then as for the second objective EC, case 2 and case 4 have a reduction with 9.1161% and 12.0977% respectively. Considering their difference in EPNL, case 4 spends less on emission and fuel consumption at the price of bringing higher noise level for the reason that the fuel consumption is less with shorter flight distance(see Tab 4). Yet this leads to a consequence of flying over an area that is sensitive to noise. Therefore, case 2 shows a capability of optimising multiple environmental impacts (e.g. noise, fuel consumption and gaseous emissions) compared with the reference trajectory.

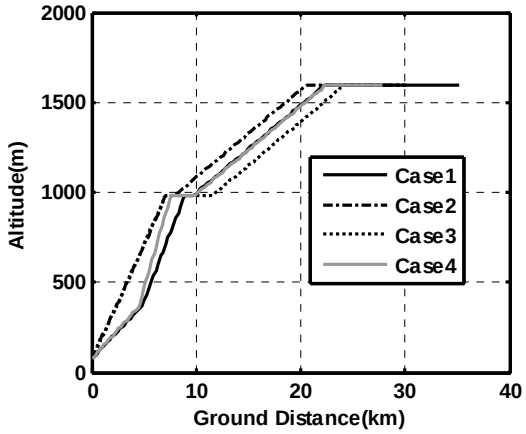

Figure 5. Altitude profile comparison

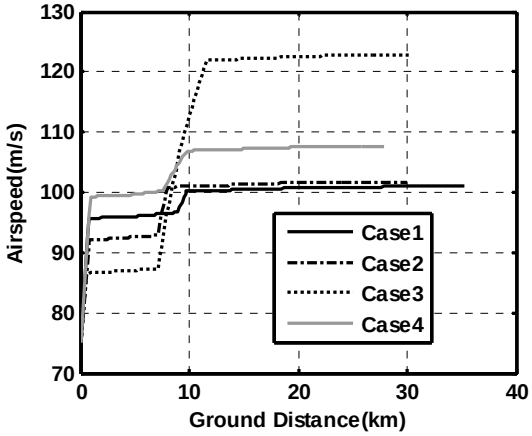

Figure 6. Airspeed profile comparison

The vertical departure procedure described in 2.2.2.2 is followed by the four cases, which can be seen in Fig. 5-6. It was founded that optimised

solutions are similar in altitude profile yet differ from each other in the airspeed profile. From the Fig 6, it follows that there is a preference towards a lower airspeed V_B during the initial climb phase before reaching 3,000 feet, which exerts a quieter operation. After passing 3,000 feet, it can be found in Fig. 6 that the influence of airspeed on the noise level is weakened due to a long distance between the receiver and the noise source.

From the analysis above, distance d is the most influential factor for the EC index in a terminal point fixed departure. Yet after comparing the airspeed profiles of case 2 and case 3 (both of which have similar ground distance (see Tab. 4)), it is indicated that lower final target speed V_D leads to lower EC.

The main reason for this is that EC is directly linked to the fuel consumption. Especially for the last part of climb, lower speed keeps the engine maintains at a less intensive working condition, which brings in less fuel burn and emissions in the end.

5. CONCLUSIONS

This paper presented the optimisation method based on genetic algorithm for departure trajectory of commercial aircraft on multiple environmental impacts on local communities around the airport. A parameterization method with dynamic bounds added for constraints is applied to discretize the dynamics models on both the vertical and lateral planes. The proposed method is tested in the departure scenario with noise, fuel consumption and emission impact considered.

In the numerical case, departure trajectory of a commercial aircraft is optimised with receptive to multiple objectives. Results show that below 3,000 feet, lower climb target speed for the initial acceleration and constant speed climb is preferred to obtain a quieter departure. Beyond 3,000 feet, lower airspeed has less impact on noise level yet is potential to reduce the cost of fuel burn and emissions. It is also concluded that detour is an effective option to avoid causing high noise level but only with the flying range limited as well. Because longer range means increased noise exposure time and more sound energy received. This also has a negative effect on emission cost criterion since the flight duration has a direct link to a growing amount of jet fuel consumption.

Future work will attempt to assess the capability of extending the proposed method to other flight phases with comprehensive operations, for example, arrival trajectory in real scenarios.

6. ACKNOWLEDGMENTS

The authors gratefully thank the financial support from the China Scholarship Council (CSC). The development of the noise prediction code was partly supported by the CleanSky Agreement 255750 (project Flight-Noise). Further information of the FLIGHT computer program is available online: www.flight.mace.manchester.ac.uk.

7. REFERENCES

1. International Civil Aviation Organisation. (2006). Procedures for Air Navigation Services, Aircraft Operations, Volume I, Flight Procedures, Fifth Edition, International Civil Aviation Organization, Technical Report Doc 8168 OPS/611.
2. International Civil Aviation Organisation. (2006) Procedures for Air Navigation Services, Aircraft Operations, Volume II, Construction of Visual and Instrument Flight Procedures, Fifth Edition, International Civil Aviation Organization, Technical Report Doc 8168 OPS/611.
3. Visser, H. G. & Wijnen, R. A. (2001). Optimization of noise abatement departure trajectories. *J. Aircr.*, 38(4), 620–627.
4. Visser, H. G. (2005). Generic and site-specific criteria in the optimization of noise abatement trajectories, *Transp. Res. Part Transp. Environ.*, 10(5), 405–419.
5. Hargraves, C. R. & Paris, S. W. (1987). Direct trajectory optimization using nonlinear programming and collocation, *J. Guid. Control Dyn.*, 10(4), 338–342.
6. Hartjes, S., Dons ,J.& Visser, H. (2014). Optimization of Area Navigation Arrival Routes for Cumulative Noise Exposure, *J. Aircr.*, 51(5), 1432–1438.
7. Prats. i Menéndez, X. (2011). Contributions to the optimisation of aircraft noise abatement procedures, degree of Doctor of Philosophy, Universitat Politècnica de Catalunya, Barcelona, Span.
8. Prats, X., Puig,V.,. Quevedo, J., & Nejjari, F. (2010). Multi-objective optimisation for aircraft

departure trajectories minimising noise annoyance. *Spec. Issue Transp. Simul. Adv. Air Transp. Res*., 18(6), 975–989.

9. Khardi, S. & Abdallah, L. (2012). Optimization approaches of aircraft flight path reducing noise: comparison of modeling methods, *Appl. Acoust*., 73(4), 291–301.

10. Torres, R., Chaptal, J., Bès,C. & Hiriart-Urruty., J.-B. (2011) Optimal, Environmentally Friendly Departure Procedures for Civil Aircraft, *J. Aircraft*., 48(1), 11–22.

11. Yu, H. & Mulder, J. A. (2011). Arrival Trajectory Optimization for Passenger Aircraft using Genetic Algorithms. In *Proc. 11th AIAA Aviation Technology, Integration, and Operations (ATIO) Conference, including the AIA*, AIAA 2011-6804, AIAA, Virginia Beach, USA.

12. Yu, H., Van Kampen, E., & Mulder, J. A. (2016). An Optimization Paradigm for Arrival Trajectories using Trajectory Segmentation and State Parameterization. In *Proc. the AIAA Guidance, Navigation, and Control Conference*, AIAA 2016-1872, AIAA, San Diego, California, USA, pp1872.

13. Hartjes, S. & Visser, H. (2016). Efficient trajectory parameterization for environmental optimization of departure flight paths using a genetic algorithm. *Proc. Inst. Mech. Eng. Part G J. Aerosp. Eng*. 954410016648980.

14. Filippone, A. (2012). *Advanced Aircraft Flight Performance*. Cambridge University Press, UK.

15. Filippone, A. (2014). Aircraft noise prediction. *Prog. Aerosp. Sci*. 68, 27–63.

16. Filippone, A. (2008). Analysis of carbon-dioxide emissions from transport aircraft. *J. Aircraft*. 45(1), 185–197.

17. Delahaye, D., Puechmorel, S., Tsiotras, P. & Feron, E. (2014). Mathematical Models for Aircraft Trajectory Design: A Survey, *Lecture notes in Electrical Engineering*. 290(5), 205-247.

18. Hasegawa, T., Tsuchiya, T. & Mori, R. (2015). Optimization of Approach Trajectory Considering the Constraints Imposed on Flight Procedure Design. *Procedia Eng*., 99, 259–267.

19. Hartjes, S., Visser, H. G., & Hebly, S. J. (2009). Optimization of RNAV Noise and Emission Abatement Departure Procedures. In *Proc. 9th AIAA Aviation Technology, Integration, and Operations Conference (ATIO)*. AIAA 2009-6953, American Institute of Aeronautics and Astronautics, Hilton Head, South Carolina, USA.

20. JEPPESEN. (2007). Airport Information EGCC(Manchester). Online at *http://www.nats-uk.ead-it.com/public/index.php%3Foption=com_content&task=blogcategory&id=99&Itemid=148.html*.

21. Manchester Airport. (2015). Runway Data Sheet: Manchester Airport Community Information. Online at: *http://www.manchesterairport.co.uk/community/living-near-the-airport/runway-data-sheet/*.

22. Deb, K., Pratap, A., Agarwal, S. & Meyarivan, T. (2002) A fast and elitist multiobjective genetic algorithm: NSGA-II. *Evol. Comput. IEEE Trans. On*, 6(2),182–197.